JOURNAL OF PHYSICAL ORGANIC CHEMISTRY, VOL. 6, 201–214 (1993)

3-METHYLCARBOXY-1*H*-INDAZOLE. THEORETICAL STUDY OF ITS FORMATION VIA INTRAMOLECULAR ALIPHATIC DIAZONIUM COUPLING AND X-RAY CRYSTAL STRUCTURE

RAINER GLASER,* CARYN L. MUMMERT AND CHRISTOPHER J. HORAN
Department of Chemistry, University of Missouri, Columbia, Missouri 65211, USA
AND
CHARLES L. BARNES*
Center for Crystallography and Department of Chemistry, University of Missouri, Columbia, Missouri 65211, USA

The methyl ester of 1*H*-indazole-3-carboxylic acid (2-Me) is formed in the diazotization of *o*-aminophenylacetic acid to *o*-diazoniumphenylacetic acid (1) in an intramolecular aliphatic diazonium coupling. 2-Me was identified and characterized by single-crystal x-ray diffraction and found to crystallize as hydrogen-bonded trimers of crystallographically independent molecules. The methylcarboxy groups are rotated slightly out of the best plane of the trimer resulting in only a pseudo-threefold axis. The crystal structure of 2-Me is compared with other indazoles and pyrazole. Regioselective electrophilic diazonium ion addition to the enol tautomer of 1 and subsequent hyrazone–azo tautomerization are proposed as a possible mechanism for indazole formation under acidic conditions. The tautomerization equilibrium between acetic acid and its enol 1,2-dihydroxyethene was studied and the effects of phenyl and *o*-diazoniumphenyl substitution on this equilibrium were explored with semi-empirical quantum mechanical methods. The performance of the semi-empirical method was assessed by comparison with *ab initio* and/or experimental data. It was found that the enol of *o*-diazoniumphenylacetic acid is stabilized greatly owing to extended conjugation and push–pull interactions in the enol form. These results suggest that the enol tautomer might be a viable reactive intermediate that warrants considerations in discussions of reaction mechanisms.

INTRODUCTION

In contrast to the well known aromatic systems, the characterization of aliphatic diazonium ions by physical organic techniques is still incomplete since they are highly reactive intermediates.[1] We have studied diazonium ions with *ab initio* theoretical methods beginning with the small aliphatic[2] and later including aromatic systems.[3] Our studies revealed that the formal charges in the commonly used Lewis structure $R—N^+\equiv N$ do not reflect the actual charge distributions. A new bonding model was proposed that is consistent with their electron density distributions and applies to all kinds of diazonium ions. We were able to establish an important link between theory and experiment recently with the first x-ray structure determinations of aliphatic diazonium ions (β,β-diethoxy-[4a] and β,β-dichlorovinyldiazonium hexachloroantimonate[4b]). Heterosubstituted diazonium ions[5,6] $(XNN)^+$ were also studied and compared with experimental data. Moreover, the bonding model was shown to be fully consistent with structural features associated with 'incipient nucleophilic attack' in diazonium ions.[7]

Crystal structures of diazonium ions with nucleophilic neighboring groups exhibit distortions that have been interpreted by postulating an 'incipient nucleophilic attack' of the proximate nucleophile on N-α. This explanation relies on the assumption that the charge distribution is correctly represented by the Lewis structure $R—N^+\equiv N$, an assumption that we have challenged. We tested the ability of our bonding model to explain the distortions in isomeric systems **A**, and the results fully support the new model.[7] Since all of the diazonium ions that we studied have rather common features, it seems reasonable to assume that our findings would carry over to the larger molecules for which experimental data exist and, hence, that the explanation for the distortions in the crystal structures

* Authors for correspondence.

0894–3230/93/040201–14$12.00

Received 21 August 1992
Revised 17 November 1992

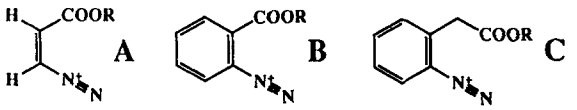

R = H, alkyl, o(r)

requires revision in general. Nevertheless, it would be advantageous to carry out the *theoretical analysis for a system for which the experimental data also exist.* Since all of the suitable known diazonium ions are too large for our *ab initio* theoretical analyses, we decided to focus on systems **B** and **C**. We have already succeeded in the determination of the crystal structures of the precursor for benzyne formation (2-carboxybenzenediazonium zwitterion hydrate),[8a] of its conjugate acid (2-diazoniumbenzoic acid)[8b] and of their 1:1 complex,[8c] and we are now focusing on the homologue **C**, which allows for more flexibility in the approach of the carboxy group toward the N_2 group. Unexpectedly, we have discovered that the title compound 3-methylcarboxy-1*H*-indazole (**2-Me**), is formed in small amounts in the synthesis of **C** (Scheme 1). We were able to obtain single crystals of this side product and to identify it by x-ray diffraction. Here, we report the crystal structure of **2-Me** and present results of a theoretical study of its formation via intramolecular aliphatic diazonium coupling. It is suggested that the heterocycle formation might involve the electrophilic diazonium ion addition to the enol form, and semi-empirical quantum-mechanical calculations were carried out and are reported to estimate the lowerings in the relative energy of the enol form of *o*-diazoniumphenylacetic acid due to the formation of the extended conjugation and to push–pull stabilization in the enol form.

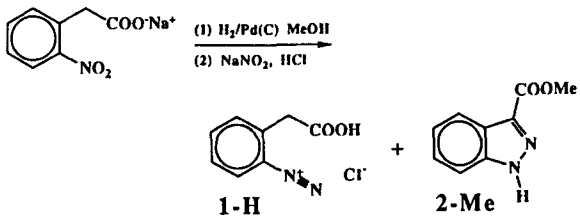

Scheme 1

EXPERIMENTAL AND THEORETICAL METHODS

Preparation. The preparation of 2-carboxymethylphenyldiazonium ion described by Baumgarten *et al.*[9] was followed. A 1·00 g (5·5 mmol) amount of 2-nitrophenylacetic acid (Aldrich) was neutralized with a solution of 331·2 mg of NaOH in 30 ml of MeOH. After addition of 10·43 mg of 10% activated Pd(C) to the acetate solution, the hydrogenation was carried out at room temperature under a hydrogen pressure of 50 psi (1 psi = 6895 Pa) for *ca* 3 h. The catalyst was removed by filtration through a layer of Celite. The solution was cooled to 0 °C and 0·381 g (5·5 mmol) of $NaNO_2$ was added to the stirred solution. A 4 ml volume of cooled HCl were added dropwise over a 7–8 min period, causing the color of the solution to become light orange. Stirring was continued for 20 min after the addition was complete. Under refrigeration, diethyl ether was allowed to diffuse into the system over a 1–1·5 day period to initiate crystallization.

Inspection of the crystals under a polarizing microscope clearly revealed the presence of two types of crystals. Aside from the needle-shaped crystals of the main product, which were unfortunately inadequate for x-ray diffraction, we found a small amount of clear hexagonal crystals of the side product 3-methylcarboxy-1*H*-indazole.

X-ray crystal structure determination. Data were collected on an Enraf–Nonius CAD4 diffractometer with graphite monochromated Cu $K\alpha$ radiation ($\lambda = 1{\cdot}5418$ Å) using the $\omega - 2\theta$ scan technique. Lattice parameters were obtained from least-squares fit of 25 reflections in the range $40 < 2\theta < 50°$. The structure was solved by direct methods with SHELXS[10] with some difficulty resulting from the strong pseudo-symmetry. Omitting several of the highest E values from the initial phase, refinement led to a correct solution. All non-hydrogen atoms were refined with anisotropic thermal parameters. All hydrogen atoms were included in the model in idealized positions with assigned isotropic thermal parameters. Assignment of the polarity of the crystal by refinement of the η parameter was not conclusive [$\eta = 2 \pm 2$]. All calculations except as noted were carried out with NRCVAX.[11] Experimental details of the x-ray analysis are given in Table 1.

Theoretical studies. The enolization of the phenylacetic acids was studied with Dewar's semi-empirical methods[12] (the program MOPAC was used[13]) and with the recent Austin Model 1 (AM1) parameter set.[14] Stewart's Parametric Model 3 (PM3)[15] also was used in a few calculations. Symmetry was imposed on some of the structures as described. All systems were optimized structurally with tight convergence criteria and the Hessian matrices were then computed to verify the stationarity of the located structure and to obtain vibrational frequencies and zero-point energies. The enolization of acetic acid was also studied with *ab initio* techniques[16] with the program Gaussian 90.[17] Structures were optimized and characterized at the RHF/3–21G level, structurally refined in optimizations at the RHF/6–31G* level and more reliable relative energies were then computed with the inclusion of perturbational corrections for electron correlation to third-

Table 1. Crystallographic data for 3-methylcarboxy-1*H*-indazole

Formula	$C_9H_8N_2O_2$	No. of data measured	4110
Formula weight	176·17	No. of unique data	1931
Space group	$P6_1$	No. of data used	1574
a (Å)	14·717(4)	R_i (merging R)	0·022
c (Å)	21·201(17)	$2q_{max}$ (°)	120
V (Å^3)	3789(3)	Range of hkl	$0 \leqslant h \leqslant 14$
Z	18		$0 \leqslant k \leqslant 13$
d_{calc} (g cm^{-3})	1·390		$0 \leqslant l \leqslant 22$
Crystal size (mm)	0·10 × 0·10 × 0·10	R^a	0·052
μ (Cu Kα) (cm^{-1})	7·6	R^b	0·062
T (°C)	23(2)	(Shift/error)$_{max}$	0·005
		Largest peak (e$^-$ Å^{-3})	0·17

[a] $R = \Sigma(|F_o| - |F_c|)/\Sigma|F_o|$.
[b] $R = [\Sigma\omega(|F_o| - |F_c|)^2/\Sigma\omega|F_o|^2]^{0.5}$, with $\omega = 1/[\sigma^2(F) + 0{\cdot}001(F^2)]$.

order in the frozen core approximation, MP3(fc)/6–31G*//RHF/6–31G*. Heats of formation, relative and vibrational zero-point energies and the *ab initio* total energies are summarized in Table 3.

RESULTS AND DISCUSSION

Solid-state structure of 3-methylcarboxy-1*H*-indazole

Figure 1 is an ORTEPII[18] view of the hydrogen-bonded trimer formed by the three crystallographically independent molecules. The pseudo-threefold axis relating the molecules is approximately parallel to the crystallographic sixfold screw axis. The H—O and H—N distances given in Figure 1 suggest probable bifurcated hydrogen bonds, although it must be noted that the hydrogen atoms were placed at calculated positions. In each molecule, the carbonyl is rotated slightly out of the plane of the indazole ring system (the torsion angle N-2—C-3—C-10—O-1 is −4·6°, −1·6° and 2·8° for molecules A, B and C, respectively).

Important bond lengths and bond angles of the 1*H*-indazole fragment of **2**-Me are listed in Table 2 for molecule A and the differences from these values in molecules B and C are also given. For comparison with the structures of other 1*H*-indazoles and of pyrazole, we selected the crystal structures of the parent indazole[19] (**3**), of 4-nitro-7-phenylsulfonylmethyl-1*H*-indazole[20] (**4**), of the indazole frameworks A and B in morpholinebis(3,5-dinitroindazole)[21] (**5**) and of di-*tert*-butyl 2-(1*H*-indazole-3-yl)aminofumarate[22] (**6**). These systems are shown in Scheme 2 [others reported with similar characteristics include 3-morpholino-6-nitroindazole,[23a] 4-(6-hydrazino-1*H*-indazol-3-yl)benzene-1,3-diol[23b] and 3-phenyl-5-methyl-1*H*-indazole[23c]].

The data in Table 2 allow one to study the responsiveness of certain bonds to substitution and/or crystal packing. Whereas **3** and **4** contain 3-unsubstituted 1*H*-pyrazoles, **5B** is closely related to **2**-Me as it contains

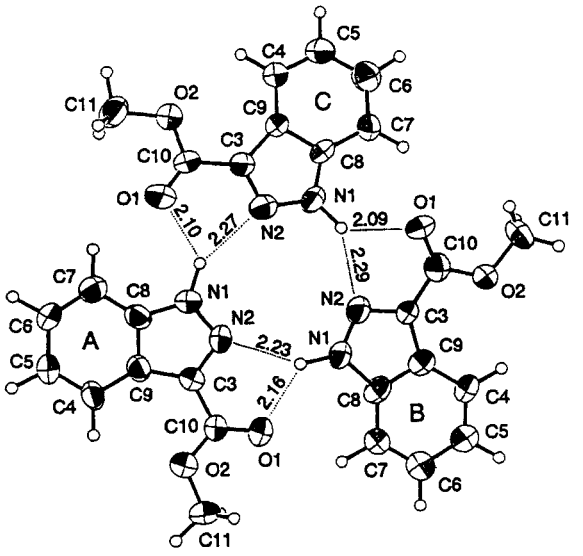

Figure 1. ORTEPII drawing of the hydrogen-bonded 3-methylcarboxy-1*H*-indazole trimer formed by the three crystallographically independent molecules

the electron-withdrawing NO_2 group in the 3-position and **6** contains an amino function (formally electron-donating) in that position. In **5B**, *a* and *d* are slightly (0·014 Å) shorter compared with **2**-Me, the pyrazole angles differ by less than 2° and the effects of the second NO_2 group are clearly manifested in the benzene ring. Except for *b*, the bond lengths in the pyrazole ring of **6** are similar to those found in **5** and the respective values for **4** also are fairly close to the values in **5**. Hence these Δ values for the pyrazole rings are not a simple consequence of the nature of the 3-substituent. Note also that most of these Δ values are no larger in magnitude than are the differences between the values determined for the symmetry-independent molecules

Table 2. Comparison of selected structural parameters with indazoles and pyrazole[a–c]

Parameter	Indazole 2-Me			Indazoles					Pyrazole 7		
	A	B (B − A)	C (C − A)	3 (Ref. 19)	4 (Ref. 20)	5 (Ref. 21) (A)	5 (Ref. 21) (B)	6 (Ref. 22)	Ref. 24 (room T)	Ref. 25 (low T)	Ref. 26 (neutron)
a	1·375	0·01	−0·013	−0·021	−0·017	−0·011	−0·013	−0·016	−0·076	−0·038	−0·042
b	1·337	−0·024	0·013	0·044	0·018	0·005	0·008	0·039	0·022	0·015	0·004
c	1·324	−0·002	−0·014	−0·036	−0·010	0·011	−0·003	−0·004	0·021	0·004	0·006
d	1·424	−0·005	0·013	−0·023	−0·012	−0·020	−0·015	−0·019	−0·086	−0·035	−0·106
e	1·396	0·021	−0·010	−0·001	0·009	0·001	0·005	0·014			
f	1·386	−0·026	−0·008	−0·033	−0·022	−0·015	−0·028	−0·013			
g	1·421	−0·040	−0·006	0·011	0·019	−0·017	−0·022	0·003			
h	1·384	−0·025	0·018	−0·025	−0·005	−0·002	−0·015	−0·010			
i	1·392	0·009	0·026	0·010	0·012	0·015	0·009	0·003			
k	1·398	−0·011	0·015	0·008	0·008	0·009	0·004	0·013	0·020	−0·027	−0·022
α_1	113·2	−1·9	−2·2	−3·1	−1·1	−5·0	−1·7	−1·2	−0·8	−0·2	−1·3
α_2	104·5	4·1	1·6	1·2	1·2	3·5	0·8	0·5	−1·5	−0·8	0·4
α_3	113·0	−4·0	0·2	0·6	−1·1	−1·1	0·1	−0·7	0·7	−1·2	−1·4
α_4	103·1	2·7	−2·0	0·7	1·0	−1·4	−0·6	1·5	0·2	2·0	1·3
α_5	106·1	−0·8	2·4	1·3	0·0	4·2	1·4	−0·2	1·5	0·2	1·2
β_1	120·3	−2·5	0·7	−2·3	−3·6	0·6	−0·1	−1·2			
β_2	118·2	0·1	−0·4	1·6	2·9	−2·5	−2·2	0·3			
β_3	119·6	4·1	2·9	0·7	0·8	4·8	4·7	1·7			
β_4	123·6	−4·8	−3·0	−2·3	−1·8	−3·5	−3·0	−2·4			
β_5	114·9	4·4	1·6	2·2	1·6	2·5	1·4	2·5			
β_6	123·4	−1·4	−1·9	−1·1	0·1	−1·8	−0·8	−0·8			

[a] Values are in Å and degrees. See Scheme 2 for definition of molecules.
[b] Differences Δ are given for molecules **3**–**6** where Δ = molecule − **2**-Me.
[c] Values for molecule A are given because they deviate the least from the average values for molecules A–C.

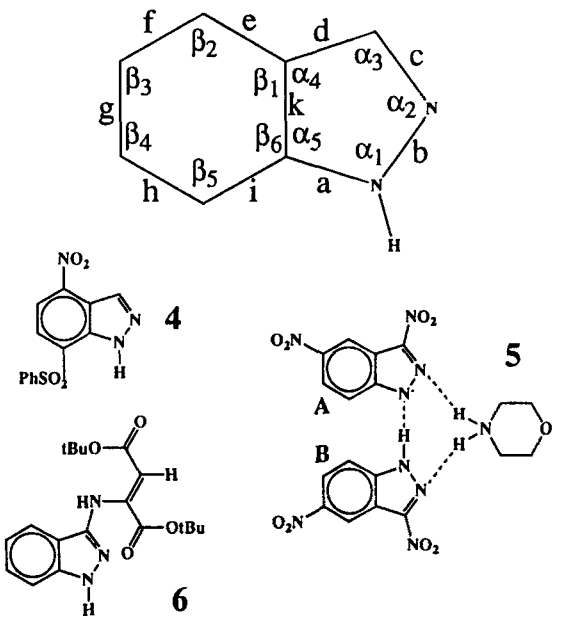

Scheme 2

A–C of **2**-Me. The parent system **3** is characterized by the longest N—N bond (1·381 Å) and comparatively short bonds *a*, *c* and *d*.

For pyrazole itself (**7**) we included entries in Table 2 for the structures determined by x-ray diffraction at room[24] and low temperature[25] and by neutron diffraction[26] [the values given in Table 2 are averaged over two independent molecules; α_1 for one of these neutron structures was reported as 120°; it appears that this value should be 112° as (i) this value agrees with the α_1 value of the second molecule in a comparable fashion as do the other values and (ii) the sum of the inner angles becomes 540°, as should be]. Note that several of the bond lengths determined in these three experiments deviate more from each other than from the respective values of the indazole **2**-Me. Considering these differences in the experimental values, we can conclude only qualitatively that benzo condensation of pyrazole lengthens bonds *d* and *a* while it shortens bonds *b* and *c* to a smaller extent.

Intramolecular aliphatic diazonium coupling

Diazonium ions are well known to couple with acidic C—H bonds of aliphatic compounds in the presence of

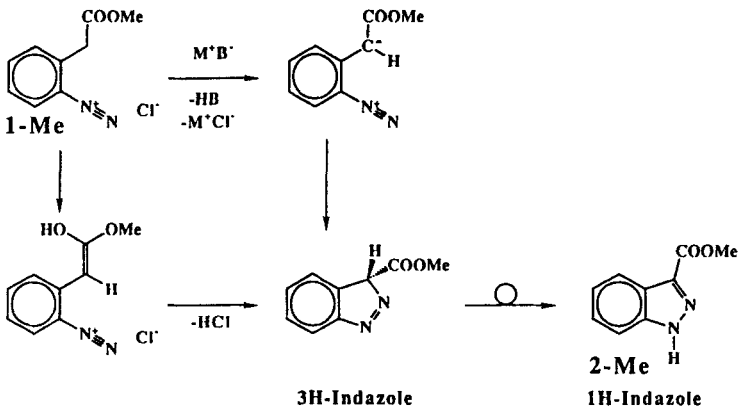

Scheme 3

a moderate base such as aqueous sodium acetate.[27,28] β-Keto-esters are typical representatives of C—H active compounds of the type Z—CH_2—Z that undergo aliphatic diazonium ion coupling (the Japp– Klingemann reaction is a special case of the aliphatic diazonium coupling, e.g. Ref. 29). In the presence of base, the mechanism most likely involves the formation of the stabilized carbanion, coupling to yield the azo compound, and subsequent tautomerization to the more stable hydrazone isomer. This base-catalyzed mechanism is outlined in Scheme 3 for the reaction of *o*-diazoniophenylmethylacetate chloride, **1**-Me. Since our crystals consist of the methyl ester of 1*H*-indazole-3-carboxylic acid, **2**-Me, we assume that a small amount of the acid, **1**-H, undergoes esterification under the acidic diazotization conditions, but it is possible that esterification occurs after the formation of the 1*H*-indazole 3-carboxylic acid, **2**-H.

Base-catalyzed diazonium coupling appears unlikely under our reaction conditions. Not only is the indazole **2** formed in the absence of base but also the methylene compound **1** shows comparatively little C—H acidity. Typical 1,3-dicarbonyls exhibit C—H acidities from 9 (1,3-diketones) to 14 (1,3-diesters), whereas esters have pK_a values of about 25. The phenyl substituent helps to increase the acidity somewhat [cf. toluene ($pK_a = 37$), Ph_2CH_2 ($pK_a = 33–35$) and Ph_3CH ($pK_a = 28–33$)[30]] but the substrate's pK_a is certainly higher than 20. According to Parmerter,[28] 'the only phenylacetic acid that has been observed to couple [intermolecularly] with diazonium salts is 2,4-dinitrophenylacetic acid' to result in formazan derivatives.

An alternative mechanism for the indazole formation may involve the addition of the diazonium ion to the enol form. This isometric enol might be formed in small amounts under the acidic conditions of diazotization and it might act as the reactive species. The respective enol is shown in Scheme 3 and its cyclization concomitant with HCl elimination yields the 1*H*-indazole, just like the base-catalyzed path, as the primary product which then tautomerizes. We have studied the equilibrium between the keto and the enol forms of **1**-H with quantum-mechanical methods to examine the feasibility of this alternative route theoretically. For the theoretical study, we select to study the acid **1**-H. Whether **1**-H or its methyl ester **1**-Me actually undergo the reaction is not clear (see above), but **1**-H provides for an excellent model in either event.

Theoretical study of the keto–enol isomerization

Judging the theoretical method

In selecting the best parameter set for our theoretical study, we reviewed the extensive compilation by Stewart.[31] Inspection of the data for aromatic systems with and without nitrogen (not including indazole) revealed no clear advantage for either AM1 or PM3. With our crystal structure of **2**-Me, however, we are now in a position to compare and judge the performance of these parameter sets with regard to our specific system of interest.

We optimized C_s symmetric **2**-Me with the AM1 and PM3 methods and the results are compared with the solid-state structure in Figure 2. As can be seen, the agreement between both theoretical methods and the x-ray data is generally very good. Bond alterations in the aromatic rings and trends in angular distortions are all manifested in the same fashion in all three data sets. There are no obvious systematic differences between calculated and measured bond lengths indicating that solid-state effects on these 'hard' parameters are very small or essentially negligible. However, angular deformations are more susceptible to packing effects as such deformations require less energy and for most angular

Table 3. Heats of formation, energies and vibrational zero-point energies[a]

Molecule	Method	ΔH_f or E	N^b	VZPE[c]	ΔE^T[d]	ΔE^T_{corr}[d]
3-Methylcarboxy-1*H*-indazole, **2**-Me						
C_s	AM1	2·36	0	103·60		
C_s	PM3	−13·99	2	98·69		
C_1	PM3	−14·36	0	98·69		
Trimer of 3-methylcarboxy-1*H*-indazole, (**2**-Me)$_3$						
C_1	AM1	−12·87			6·65[e]	
Planar	AM1	−12·89				
C_1	PM3	−57·18			4·70[e]	
Planar	PM3	−57·21				
Acetic acid isomers						
8a, eclip. OH	AM1	−103·02	0	39·00	20·00	20·79
	RHF/3–21G	−226·532925	1	41·30		
8b, stag. OH	AM1	−102·99	1	38·91		
	RHF/3–21G	−225·534237	0	41·39	26·38	25·88
	RHF/6–31G*	−227·810648			35·42	34·92
	MP2(fc)/6–31G*	−228·415423			36·10	
	MP3(fc)/6–31G*	−228·427686			33·20	
9a, *cis–tr*	AM1	−83·02	0	39·79		
	RHF/3–21G	−226·492201	0	40·84		
	RHF/6–31G*	−227·754194				
	MP2(fc)/6–31G*	−228·357892				
	MP3(fc)/6–31G*	−228·374773				
9b, *cis–cis*, C_s	AM1	−79·35	0	39·65		
9c, *tr–tr*, C_{2v}	AM1	−77·27	1	37·65		
9d, *tr–tr*, C_2	AM1	−80·66	1	37·96		
9e, *tr–tr*, C_s	AM1	−78·05	1	37·67		
2′-Diazonium-phenylacetic acid isomers						
10a, C_s	AM1	158·99	2	91·07	3·28	3·34
11a, C_s	AM1	162·27	1	91·13		
10b, C_1, HO_{pr}	AM1	151.68	0	91·68		
10c, C_1, CO_{pr}	AM1	149.15	0	91·72	7·98	
11b, C_1	AM1	162·17	0	90·65		
11c, C_1	AM1	157·13	0	91·34		
Phenylacetic acid isomers						
12a, C_s	AM1	−71·74	2	91·86	17·56	16·38
13a, C_s	AM1	−54·18	2	90·68		
12b, C_1	AM1	−75·47	0	92·18	14·49	14·13
13b, C_1	AM1	−60·98	0	91·82		

[a] Values in kcal mol^{-1} except for *ab initio* total energies which are in atomic units.
[b] Number of imaginary frequencies NIMAG.
[c] Vibrational zero-point energy.
[d] Relative stability of the keto over the enol form without and with inclusion of vibrational zero-point energy corrections.
[e] These values are trimerisation energies for **2**-Me in kcal mol^{-1} per indazole unit.
[f] Møller–Plesset calculations based on RHF/6–31G* structures.

parameters we find that the sets of calculated parameters differ less among each other than compared to the experimental data. The most noticeable differences occur in the C—N—N(H) (α_2) and C—C—N (α_3) angles of the pyrazole; in the solid state the N—N—N(H) angle is compressed to 104·5° and C—C—N angle is opened to 113·0° whereas the calculated values indicate only small deviations from the ideal five-membered ring angle of 108°. The angles in the pyrazole ring of **2**-Me are in excellent agreement with the respective values found in crystal structures of the indazoles and pyrazole (see above). Since the packing effects for **2**-Me and the crystals of the other indazoles and of pyrazoles are all different, it would appear that the deviations in the angles C—C—N and C—N—N(H) indicated by the theoretical methods are artifacts of the methods.

The Hessian matrices were calculated for the C_s structures to assure that the stationary structures are minima. The AM1 optimized structure was confirmed to be a minimum, but two imaginary frequencies were found for the PM3 structure. Both of these imaginary

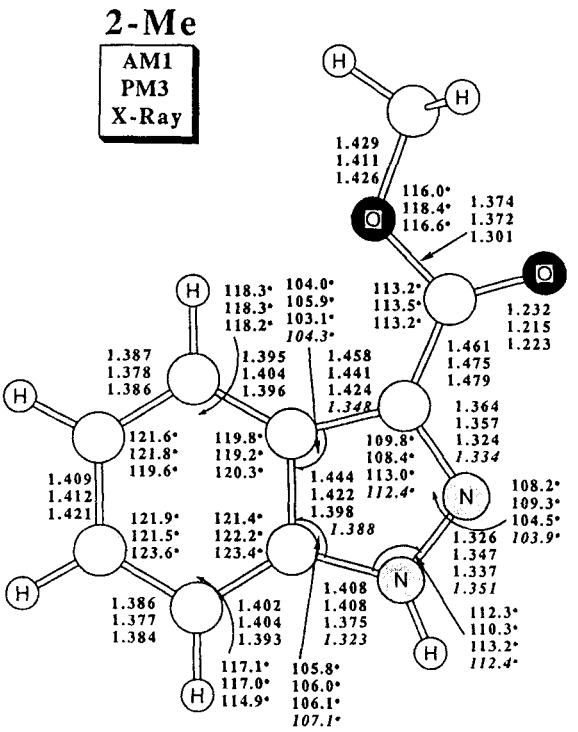

Figure 2. Selected structural parameters of 3-methylcarboxy-1*H*-indazole as determined with AM1 and PM3 compared with values determined in the x-ray diffraction study. Values given by italics are the averages of the experimental values for pyrazole; compare Table 2

frequencies are *a''*-symmetric and the associated transition vectors indicate pyramidalization at the NH-nitrogen (i138 cm^{-1}) and a torsion of the methylcarboxy group (i25 cm^{-1}). We reoptimized the indazole with the PM3 parameters without any constraints and found a chiral minimum that is only 0·4 kcal mol^{-1} (1 kcal = 4·184 kJ) more stable than the planar structure. This chiral structure differs very little from the planar structure: only the torsional parameters are affected. Specifically, the carboxyl group is rotated significantly with respect to the indazole plane by 47° and the pyrazole-1N is pyramidalized such that a 1H—N—N—C dihedral angle of 160° results. [We note that the potential energy surfaces along the N-1 inversion path are rather shallow on the AM1 and on the PM3 surfaces. The frequencies of the vibrational modes corresponding to pyramidalization (AM1) or N inversion (PM3) all are $\ll 100\ cm^{-1}$.] These results suggest that PM3 underestimates the degree of electron delocalization in the pyrazole ring to some extent and AM1 was therefore used in study of the enolization equilibria.

Trimerization of 3-methylcarboxy-1H-indazole

We optimized (2-Me)$_3$ at the semi-empirical levels completely and also with the condition that the indazoles all lie in the same plane. While the complete optimizations resulted in chiral structures of the type found in the solid state, the heats of formation (Table 3) suggest no intrinsic advantage for asymmetric structures and, importantly, they also show that such small distortions require very little energy.

The C_s-optimized and *de facto* C_{3v} AM1 structure of (2-Me)$_3$ is shown in Figure 3. The crystal structure analysis indicates bifurcated H-bonds with the H—O bond being longer than the H—N bond by about 0·17 Å (Figure 1). The PM3 structure exhibits such bifuraction and the same preference for shorter H—O bonds compared with N—H bonds (by 0·18 Å) but all H-bond lengths are predicted to be much longer (*ca* 0·4 Å). In contrast, the AM1 structure shows a clear preference for the O-acceptor: the H—O distances are 2·12 Å and agree closely with the x-ray structure but the H—O and H—N distances differ greatly (by 0·62 Å). With the AM1 and PM3 parameters, the trimerization energies, that is the stability increase for each 2-Me upon trimer formation, are 6·7 (AM1) and 4·7 (PM3) kcal mol^{-1}, respectively.

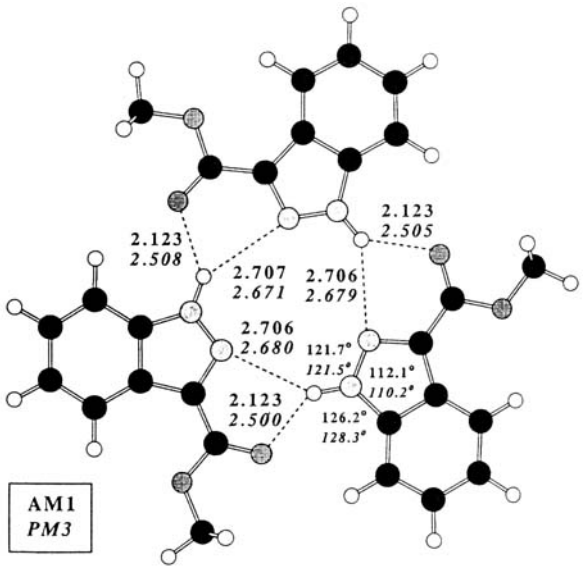

Figure 3. Selected structural parameters of the C_s symmetric hydrogen-bonded trimer of 3-methylcarboxy-1*H*-indazole as determined with AM1 and PM3

Acetic acid enolization

Enolizations of carbonyls and the keto–enol equilibrium of acetaldehyde in particular have been studied

in detail both theoretically[32-34] and experimentally,[35] but there are only a few reports on the corresponding process for carboxylic acids (the radical cations of acetic acid and its enol forms have been studied in the gas phase[36a] and substituent effects were examined theoretically[36b]) or derivatives (for a recent example, see Ref. 37. Enolization is considered to be the key step in the conversion of arylacetohydroxamic acids to secondary amides. It is thought that a conjugating group at C-2 is needed to acidify the α-proton or to increase the proportion of the enol form). For acetaldehyde, the enol form vinyl alcohol was calculated to be 13 kcal mol^{-1} less stable at levels that employed double-ζ basis sets and included electron correlations.

Acetic acid was optimized with the AM1 method with the CH_3 group either eclipsing (**8a**) or staggering (**8b**) the HO group. Conformation **8a** is the minimum and **8b** is the transition state structure for the nearly free CH_3 rotation. Several isomers of the enol form 1,1-dihydroxyethene (**9**) were examined (Figure 4). The planar structure **9a** in which the conformations about the C—O bonds are *cis* and *trans* is the most stable one for **9**. Structure **9b** with two C—O *s-cis* conformations

also is a minimum 3·7 kcal mol^{-1} higher in energy. Three structures with two C—O *s-trans* conformations were considered within different symmetry constraints, but each one of these exhibits one imaginary frequency (Figure 4) and thus they all are transition-state structures. With the most stable isomers **8a** and **9a**, the heat of reaction for the enolization reaction is 20·0 kcal mol^{-1}. Inclusion of the vibrational zero-point energy differences increases the endothermicity of this equilibrium by about 0·8 kcal mol^{-1}.

At the RHF/3–21G level, the energy difference between **8a** and **8b** remains small (0·8 kcal mol^{-1}) but is in favor of **8b**. Of the enol forms, only **9a** was considered at the *ab initio* RHF/3–21G level and it was confirmed as a minimum. Forms **8b** and **9a** were re-optimized at RHF/6–31G* (Figure 4) and the effects of electron correlation on relative isomer stability were estimated with third-order Møller–Plesset

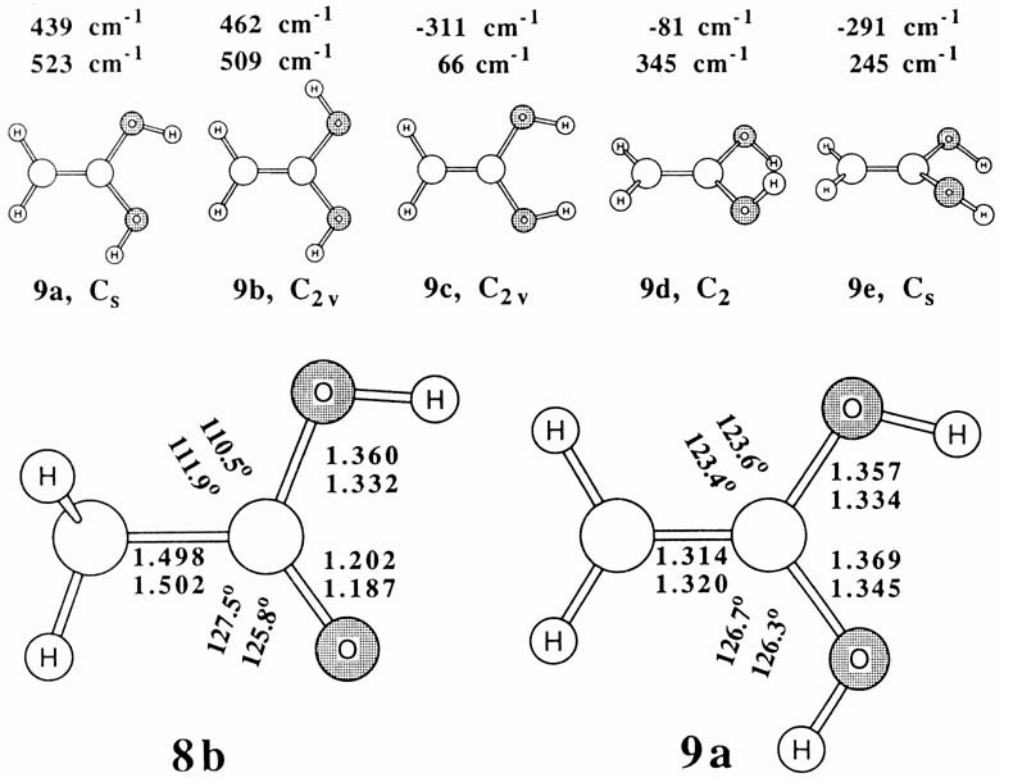

Figure 4. Enolization of acetic acid. AM1 optimized stationary structures are shown on top together with their symmetries and the frequencies of the two lowest vibrations. The *ab initio* structures are shown in more detail with structural parameters given at the levels RHF/3–21G and RHF/6–31G*

perturbation theory. At our highest level, MP3(fc)/6–31G*//RHF/6–31G*, we find a preference of 33·2 kcal mol^{-1} for the keto form **8b** of acetic acid compared with the enol form **9a**. Vibrational zero-point energy corrections reduce this preference (after scaling) by 0·5 kcal mol^{-1}. The enolization of acetic acid thus requires about 20 kcal mol^{-1} more energy compared with the formation of vinyl alcohol from acetaldehyde. The *ab initio* data indicate that the absolute preference energies for the acid are underestimated by the semi-empirical theory. In reflection of this finding, our discussion of the semi-empirical results for the much larger systems will focus more on relative lowerings in the preference energies than on their absolute values. The semi-empirical theory is well known to reproduce such relative energy differences much more reliably.

Enolization of o*-diazoniumphenylacetic acid*

To estimate the effects of the aromatic ring system on the enolization equilibrium pertinent to the formation of the indazole 2-Me, we considered the cation *o*-diazoniumphenylacetic acid, **10**, and its enol form, **11**, in our AM1 study. The planar structures of **10a** and **11a**

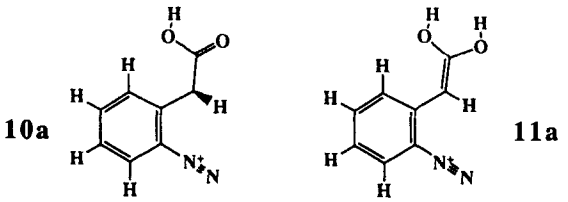

were first optimized with the assumed stereochemistries shown. Both of these structures either are transition states or higher order saddle points. Optimization of **10** without symmetry constraints resulted in the structure **10b**, shown in Figure 5, in which the hydroxyl O-atom is placed in proximity to the N_2 function. Rotamer **10c** in which the carbonyl-O is close to the N_2 group was also optimized. Unconstrained reoptimization of **11a** resulted in the chiral structure **11b** shown in Figure 6 and the rotamer **11c** also was found as a minimum. As with the parent 1,1-dihydroxyethene, the *cis–trans* conformations about the C—O bonds are preferred; **11c** is 5·0 kcal mol^{-1} more stable than **11b**.

In **10b** and **10c**, the carboxyl groups are oriented in such a fashion as to allow for electrostatically favourable neighboring group interactions with the diazonium function. We have discussed the nature of these interactions in detail for the smaller system 3-diazoniumpropenoic acid[7] and, recently, we have applied our new electrostatic analysis method to 2′-diazoniumbenzoic acid and 2′-diazoniumbenzoate with equal success.[38] This electrostatic model predicts a higher stability for the conformation that places the more highly charged oxygen in the proximity of the diazonium function. As expected, **10c** with its carbonyl-O close to the N_2 function is preferred by 2·5 kcal mol^{-1} over **10b**.

With the most stable structures of the keto form (**10c**) and of the enol form (**11c**) of *o*-diazoniumphenylacetic acid, we find that the enol is only 8·0 kcal mol^{-1} higher in energy than the acid. The *o*-diazonium phenyl substituent lowers the relative energy of the enol form by the substantial amount of 12 kcal mol^{-1}. Our theoretical results suggest that the enol might indeed be a viable intermediate and that it might be the reactive species involved in the aliphatic diazonium coupling as proposed in Scheme 3. The addition of aromatic diazonium ions to activated double bonds is well documented.[28] In contrast to the well known Widman–Stoermer synthesis[39] of cinnolines via the diazotization of *o*-aminophenylethenes, the addition to the enol form of the ester would undoubtedly prefer the regiochemical route leading to the pyrazole rather than the pyridazine formation.

Enolization of phenylacetic acid

The enolization of the parent phenylacetic acid was examined to quantitatively estimate the magnitude of the diazonium substituent effect on the enolization equilibrium. We first optimized the planar structures of **12a** and **13a** with the assumed stereochemistries as in the case of **10** and **11** and then optimized the chiral minima **12b** and **13b** without symmetry constraints. Structures of **12b** and **13b** are shown in Figure 7. According to the AM1 heats of formation, the enol form **13b** is 14·5 kcal mol^{-1} less stable than the keto form **12b**.

The assistance of the electron-withdrawing diazonium function is clearly important for the enolization of the *o*-diazoniumphenylacetic acid. The heat of reaction for enolization of the diazonium ion system is 6·5 kcal mol^{-1} less compared to the unsubstituted phenylacetic acid. Not only does enolization provide the advantage of conjugative stabilization through the formation of the phenylvinyl system (mesomeric form **I**) but, in addition, the highly electron-withdrawing N_2-substituent causes push–pull electron density shifts that stabilize the enol form through partial delocalization of the positive charge on to the dihydroxyvinyl substituent as represented formally by the mesomeric forms **II** and **III**.

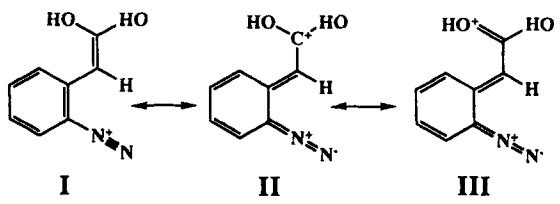

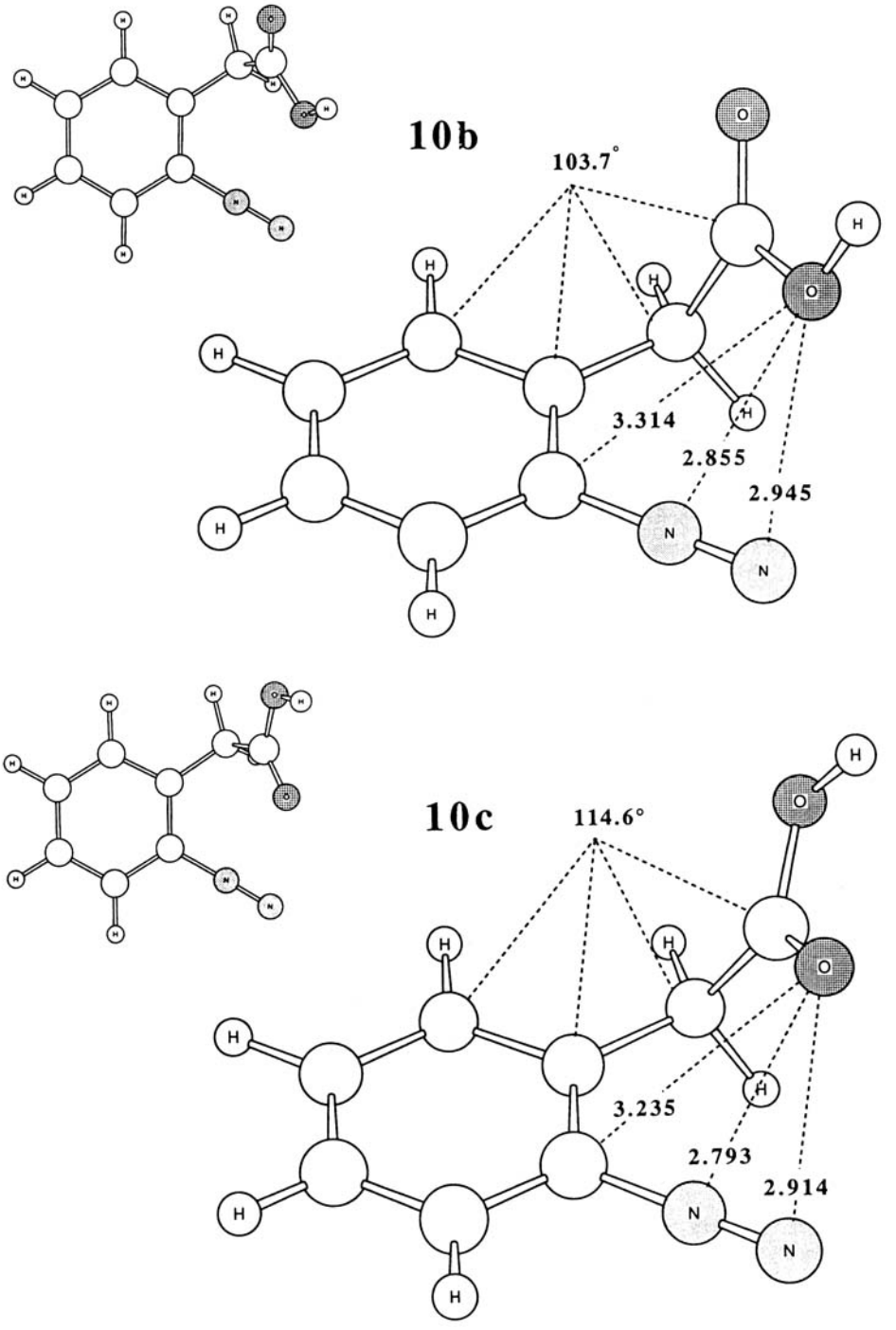

Figure 5. Rotamers of *o*-diazoniumphenylacetic acid as optimized with the AM1 model. **10c** is preferred over **10b**

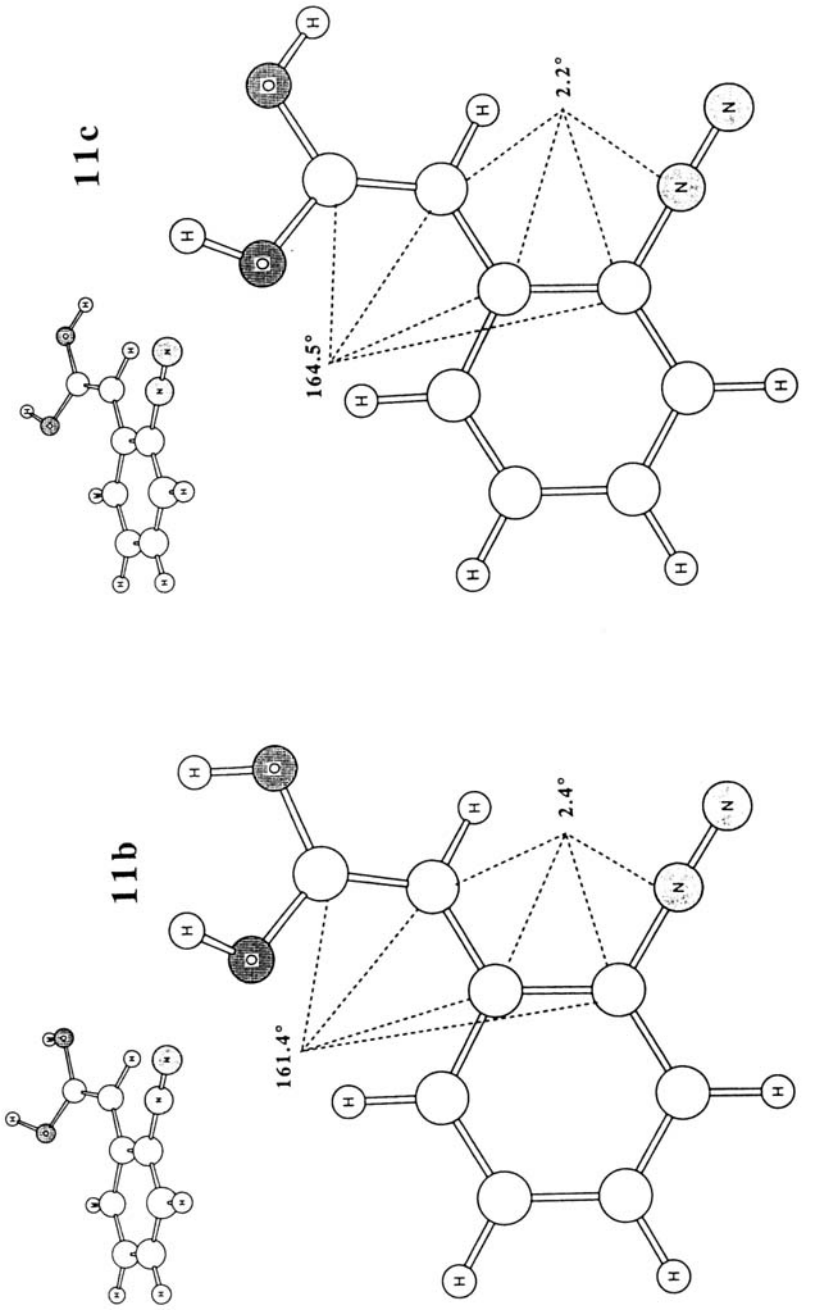

Figure 6. AM1 optimized structures of the enol form of *o*-diazoniumphenylacetic acid, **11**. Rotamer **11c** is preferred over **11b**

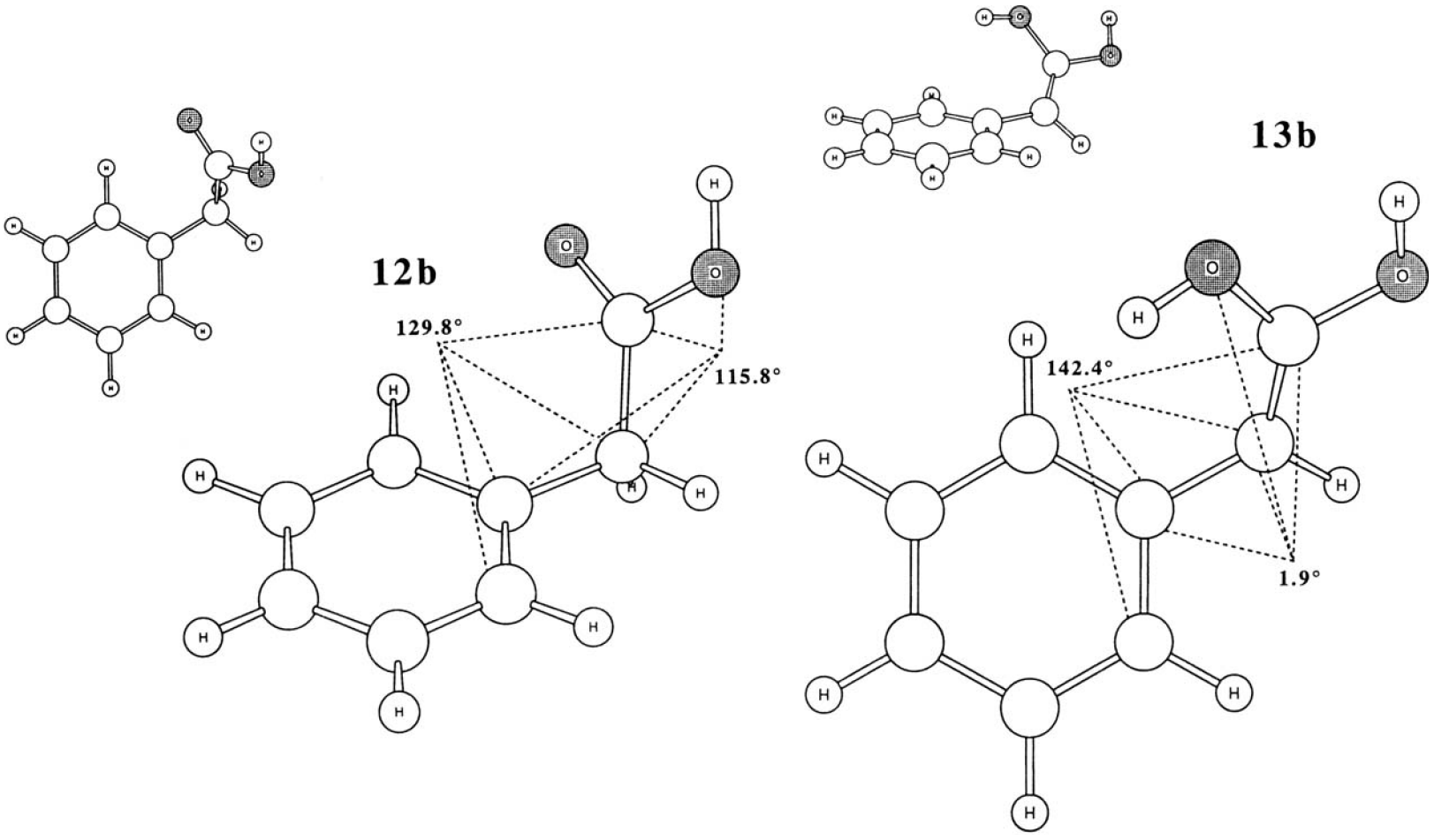

Figure 7. AM1 optimized structures of phenylacetic acid, **12b**, and of its enol form, **13b**

CONCLUSION

3-Methylcarboxy-1*H*-indazole, **2**-Me, is formed by *intra*molecular aliphatic diazonium coupling in the diazotization of *o*-aminophenylacetic acid was identified and structurally characterized by single-crystal x-ray crystallography. Whereas intermolecular aliphatic diazonium coupling was reported for the one case of 2,4-dinitrophenylacetic acid, the intramolecular coupling to a methylene group of low acidity in the absence of base appears unprecedented.

It is proposed that indazole formation might involve the addition of the diazonium function in a regioselective fashion to the enol form of the substrate. Additions of diazonium ions to activated C=C double bonds are precedented and our semi-empirical studies suggest that the enol form of *o*-diazoniumphenylacetic acid is a viable species that might be the reactive species. With the AM1 parameters, the semi-empirical calculations suggest that the enolization of acetic acid is greatly assisted by the *o*-diazoniumphenyl substituent and that the enol is only about 8 kcal mol^{-1} higher in energy compared with the acid. Our higher level *ab initio* calculations suggest that the AM1 method overestimates the stability of the enol somewhat, but the qualitative conclusions are expected to remain valid. The comparison with the enolization of phenylacetic acid itself shows that both the formation of the extended conjugated system as well as push–pull stabilization are equally important for the relative stabilization of the enol form.

The diazotization of *o*-aminophenylacetonitrile under the same conditions yield 3-cyanoindazole in good yield[40] (note that the acid **1**-H is accessible synthetically by hydrolysis of the product 3-cyanoindazole). The mechanism of that reaction has not been studied and it remains an open question whether an analogous 'enolization' might be involved. Substituted *o*-toluidines form indazoles in good yield[41] via intramolecular aliphatic diazonium coupling. Again, the mechanism of this reaction is not known, although it obviously must be different from the one discussed here for the phenylacetic acids.

Supplementary material is available directly from the authors and contains structure factors, positional parameters, an isotropic thermal parameters and intra- and intermolecular bond lengths and angles (10 pages) together with archive entries of the semi-empirical and *ab initio* calculations (26 pages). Further details of the crystal structure investigation are available on request from the Director of the Cambridge Crystallographic Data Centre, University Chemical Laboratory, Lensfield Road, Cambridge CB2 1EW, UK, on quoting the full journal citation.

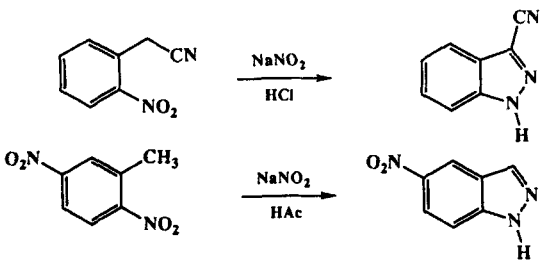

ACKNOWLEDGEMENTS

Acknowledgment is made to the Donors of the Petroleum Research Fund (PRF No. 24399-G4), administered by the American Chemical Society, and to the MU Research Council (92-RC-023-BR) for support of this research. C.L.M. gratefully acknowledges support through a Howard Hughes Undergraduate Research Internship. C.J.H is the recipient of a Dorothy Nightingale Fellowship and he also thanks ABC Laboratories for a Graduate Research Fellowship. The x-ray diffractometer was partially funded by the National Science Foundation (CHE-9011804).

REFERENCES

1. Reviews: (a) W. Kirmse, *Angew. Chem., Int. Ed. Engl.* **15**, 251 (1976); (b) K. Laali and G. A. Olah, *Rev. Chem. Intermed.* **6**, 237 (1985).
2. (a) R. Glaser, *J. Phys. Chem.* **93**, 7993 (1989); (b) R. Glaser, G. S.-C. Choy and M. K. Hall, *J. Am. Chem. Soc.* **113**, 1109 (1991).
3. (a) R. Glaser, *J. Comput Chem.* **11**, 663 (1990); (b) R. Glaser and C. J. Horan, in preparation.
4. R. Glaser, G. S. Chen and C. L. Barnes, (a) *Angew. Chem.* **104**, 749 (1992); (b) in preparation.
5. (a) R. Glaser and G. S.-C. Choy, *J. Phys. Chem.* **95**, 7682 (1991); (b) R. Glaser, G. S.-C. Choy and C. J. Horan, *J. Org. Chem.* **57**, 995 (1992).
6. (a) F. Cacace, M. Attina, G. De Petris, F. Grandinetti and M. Speranza, *Gazz. Chim. Ital.* **120**, 691 (1990); (b) R. Glaser and G. S.-C. Choy, *J. Org. Chem.* **57**, 4976 (1992).
7. R. Glaser, C. J. Horan, E. Nelson and M. K. Hall, *J. Org. Chem.* **57**, 215 (1992).
8. (a) C. J. Horan, C. L. Barnes and R. Glaser, *Chem. Ber.* in press; (b) C. J. Horan, C. L. Barnes and R. Glaser, *Acta Crystallogr.* in press; (c) C. J. Horan, P. Haney, C. L. Barnes and R. Glaser, *Acta Crystallogr.* submitted for publication.
9. H. E. Baumgarten, P. L. Creger and R. L. Zey, *J. Am. Chem. Soc.* **82**, 3977 (1960).
10. G. M. Sheldrick, in *Crystallographic Computing 3*, edited by G. M. Sheldrick, C. Kruger and R. Goddard, pp. 175–189. Oxford University Press, Oxford (1985).
11. E. J. Gabe, Y. Le Page, J.-P. Charland and F. L. Lee, *J. Appl. Crystallogr.* **22**, 384 (1989).
12. M. J. S. Dewar and W. Thiel, *J. Am. Chem. Soc.* **99**, 4899 (1977).
13. J. J. P. Stewart, *QCPE* No. 455, Vax/VMS Version 5.0.

14. M. J. S. Dewar, E. G. Zöbisch, E. F. Healy and J. J. P. Stewart, *J. Am. Chem. Soc.* **107**, 3902 (1985).
15. J. J. P. Stewart, *J. Comput. Chem.* **10**, 221 (1989).
16. W. J. Hehre, L. Radom, P. v. R. Schleyer and J. A. Pople, *Ab Initio Molecular Orbital Theory*. Wiley, New York (1986).
17. M. J. Frisch, M. Head-Gordon, G. M. Trucks, J. B. Foresman, H. B. Schlegel, K. Raghavachari, M. A. Robb, J. S. Binkley, C. Gonzales, D. J. Defrees, D. J. Fox, R. A. Whiteside, R. Seeger, C. F. Melius, J. Baker, R. L. Martin, L. R. Kahn, J. J. P. Stewart, S. Topiol and J. A. Pople, *Gaussian 90*. Gaussian, Pittsburgh, PA (1990).
18. C. K. Johnson, *ORTEPII*. Report ORNL-5138, Oak Ridge National Laboratory, Oak Ridge, TN (1976).
19. A. Escande and J. Lapasset, *Acta Crystallogr., Sect. B* **30**, 2009 (1974).
20. A. Gzella, V. Wrzeciono, J. Dudzinska-Usarewicz and T. Borowiak, *Acta Crystallogr., Sect C* **45**, 642 (1989).
21. A. Gzella, V. Wrzeciono and T. Borowiak, *Acta Crystallogr., Sect. C* **45**, 644 (1989).
22. I. Leban, L. Golic and S. Polanc, *Acta Crystallogr., Sect. C* **43**, 2455 (1987).
23. T. Borowiak and M. Gawron, *Acta Crystallogr., Sect. A* **40**, C100 (1984); (b) R. Krishnan, S. A. Lang, J. L. Yang-i and R. G. J. Wilkinson, *Heterocycl. Chem.* **25**, 447 (1988); (c) A. A. Dvorkin, A. S. Javorskii, Yu. A. Simonov, G. E. Golodeev, S. A. Andronati and T. I. Malinovskii, *Dolk, Akad. Nauk SSSR* **305**, 1378 (1989).
24. H. W. W. Ehrlich, *Acta Crystallogr.* **13**, 946 (1960).
25. T. La Cour and S. E. Rasmussen, *Acta Chim. Scand.* **27**, 1845 (1973).
26. K. F. Larsen, M. S. Lehman, I. Søtofte and S. E. Rasmussen, *Acta Chim. Scand.* **24**, 3248 (1970).
27. J. March, *Advanced Organic Chemistry*, 3rd ed., pp. 532*ff*. Wiley, New York (1985).
28. Review: S. M. Parmerter, *Org. React.* **10**, 1 (1959).
29. (a) R. R. Phillips, *Org. React.* **10**, 143 (1959); (b) H. C. Yao and P. Resnick, *J. Am. Chem. Soc.* **84**, 3514 (1962).
30. H. O. House, *Modern Synthetic Reactions*, p. 494. Benjamin/Cummings, Menlo Park, CA (1972).
31. J. J. P. Stewart, *J. Comput.-Aided Mol. Des.* **4**, 1 (1990).
32. B. Capon, D. S. Rycroft, T. W. Watson and C. Zucco, *J. Am. Chem. Soc.* **103**, 1761 (1981).
33. W. J. Bouma, D. Poppinger and L. Radom, *J. Am. Chem. Soc.* **99**, 6444 (1977).
34. W. R. Rodwell, W. J. Bouma and L. Radom, *J. Quantum Chem.* **18**, 107 (1980).
35. A. L. Bertran and O. N. Ventura, *Int. J. Quantum Chem.* **30**, 467 (1986).
36. (a) J. L. Holmes and F. P. Lossing, *J. Am. Chem. Soc.* **102**, 3732 (1980); (b) N. Heinrich, W. Koch, G. Frenking and H. Schwarz, *J. Am. Chen. Soc.* **108**, 593 (1986).
37. R. V. Hoffman, N. K. Nayyar and B. W. Klinekole, *J. Am. Chem. Soc.* **114**, 6262 (1992).
38. R. Glaser and C. J. Horan, in preparation.
39. (a) O. Widman, *Chem. Ber.* **17**, 722 (1884); (b) R. Stoermer and O. Gaus, *Chem. Ber.* **45**, 3104 (1912).
40. (a) R. Pschoor and G. Hoppe, *Chem. Ber.* **43**, 2543 (1910).
41. E. Nölting, *Chem. Ber.* **37**, 2556 (1904).